SIRT-1 is required for release of enveloped picornaviruses

Alagie Jassey, James Logue, Stuart Weston, Michael A. Wagner, Ganna Galitska, Katelyn Miller, Matthew B. Frieman, and William T. Jackson*

1. Department of Microbiology and Immunology and Center for Pathogen Research, University of Maryland School of Medicine, 685 W. Baltimore Avenue, Baltimore, MD 21201, USA

*Corresponding Author and Lead Contact: Email: wjackson@som.umaryland.edu

ABSTRACT

Enterovirus D68 is a re-emerging enterovirus that causes acute respiratory illness in infants and has recently been linked to Acute Flaccid Myelitis. Here, we show that the histone deacetylase, SIRT-1, is essential for autophagy and EV-D68 infection. Knockdown of SIRT-1 blocks autophagy and reduces EV-D68 extracellular titers. The proviral activity of SIRT-1 does not require its deacetylase activity or functional autophagy. SIRT-1's proviral activity is, we demonstrate, mediated through the repression of ER stress. Inducing ER stress through thapsigargin treatment or SERCA2A knockdown in SIRT-1 knockdown cells had no additional effect on EV-D68 extracellular titers. Knockdown of SIRT-1 also decreases poliovirus and SARS-CoV-2 titers but not coxsackievirus B3. In non-lytic conditions, EV-D68 is primarily released in an enveloped form, and SIRT-1 is required for this process. Our data show that SIRT-1, through its translocation to the cytosol, is critical to promote the release of enveloped EV-D68 viral particles.

INTRODUCTION

Enterovirus D68 (EV-D68) is a re-emerging enterovirus and a cause of acute respiratory illness in infants. EV-D68 infection has recently been associated with Acute Flaccid Myelitis, a severe polio-like neurological disease that causes limb weakness and loss of muscle tone in infants(Eshaghi et al., 2017; Lang et al., 2014). There is currently no FDA-approved drug or vaccine against EV-D68. It is important to understand how EV-D68 hijacks host processes to facilitate its life cycle within the host.

EV-D68 is a positive-sense single-stranded RNA enterovirus belonging to the *Piconarviridae* family. The viral genome encodes a single polyprotein that is immediately processed upon translation by viral proteases into multiple intermediate and mature structural and seven non-structural proteins(Esposito et al., 2015). Picornavirus infection induces extensive rearrangement of cytosolic membranes, beginning with the formation of complex single convoluted membranes, also known as replication vesicles, on the cytosolic face of which viral RNA replication occurs. For most picornaviruses, these intricate structures eventually morph into double-membrane autophagosome-like structures, which play roles in virus replication, maturation, and nonlytic release(Jackson, 2014; Jackson et al., 2005; Shi and Luo, 2012).

Autophagy is a highly regulated catabolic process that maintains cell survival by targeting superfluous cytoplasmic contents and infectious microorganisms, including pathogenic bacteria and viruses, for degradation. Several RNA viruses, including EV-D68, are known to subvert autophagy for their own benefit, and our interest in this

pathway led us to study sirtuin 1 (SIRT-1)(Ahmad et al., 2018). SIRT-1 is important for autophagy initiation, but whether SIRT-1 is essential for the later stages of autophagy (autophagic flux) or translocates to the cytosol during starvation or other stress stimuli, such as viral infection, is unknown(Bai and Zhang, 2016; Huang et al., 2015; Lee et al., 2008). A growing body of evidence implicates SIRT-1 as an essential regulator of autophagy downstream of the nucleation complex(Green and Levine, 2014; Huang et al., 2015; Lee et al., 2008).

SIRT-1 belongs to the NAD^+-dependent family of histone deacetylase enzymes, which are known to control several physiological processes. The sirtuin family of enzymes contains seven members (SIRT-1 to 7), which display varying subcellular localization, with SIRT-1 being the most studied owing to its role in lifespan expansion(Chalkiadaki and Guarente, 2015; Jing and Lin, 2015). SIRT-1 has been shown to regulate cellular responses to various stresses, including the cell cycle, apoptosis, inflammation, ER stress, and more(Chalkiadaki and Guarente, 2015). SIRT-1 has also been shown to promote the Middle East respiratory syndrome coronavirus infection, but whether SIRT-1 regulates picornavirus infection is unknown(Weston et al., 2019).

A less well-known or studied role for SIRT-1 is in regulating Endoplasmic Reticulum stress (ER stress)(Li et al., 2014; Singh et al., 2020; Tang et al., 2018). ER stress, which can be provoked by various stress stimuli, including viral infection, happens when proteins cannot properly fold, leading to the accumulation of unfolded/misfolded protein. ER stress engages the unfolded protein response (UPR), which attenuates transcription

and translation, decreases protein synthesis, and enhances the expression of molecular chaperones to increase the cell's protein folding capacity(Oslowski and Urano, 2011). The inositol-requiring enzyme (IRE) 1-X-box binding protein (XBP) 1 pathway constitutes one of the three major pathways induced by UPR(Hetz, 2012). Upon ER stress, IRE-1 cleaves XBP-1 mRNA into spliced forms which, in turn, activates UPR target genes(Yoshida et al., 2001). Studies have shown an intricate interplay between SIRT-1 and ER stress. While SIRT-1 regulates ER stress by binding and inhibiting the transcriptional activity of XBP1, ER stress also regulates SIRT-1 levels(Wang et al., 2011). For instance, ER stress induction through Thapsigargin (TG) treatment induces SIRT-1 protein levels *in vivo* and *in vitro* to promote hepatocellular injury(Koga et al., 2015).

Here, we report that EV-D68 infection induces SIRT-1 translocation to the cytosol. We also show that SIRT knockdown impedes the extracellular vesicle-mediated release of infectious EV-D68 particles. We further demonstrate that the pro-EV-D68 activity of SIRT-1 is mediated through repressing ER stress and does not require SIRT-1's deacetylase function, nor is it dependent on functional autophagy. Moreover, SIRT-1 knockdown reduces extracellular titers of poliovirus (PV) and SARS-CoV-2 but not Coxsackievirus B3 (CVB3). Our results indicate that certain picornaviruses induce SIRT-1 translocation to the cytosol and require the cellular protein for efficient release.

RESULTS

EV-D68 infection changes SIRT-1's subcellular localization

SIRT-1 is proviral in some cases and has previously been reported to regulate autophagy initiation, which is important for EV-D68 infection(Huang et al., 2015; Lee et al., 2008; Weston et al., 2019). But whether SIRT-1 is essential for EV-D68 reproduction is unknown. We first interrogated the effects of SIRT-1 knockdown on EV-D68 titers. SIRT-1 knockdown reduced both the intracellular (Fig. 1A) and extracellular (Fig. 1B) EV-D68 titers, with the knockdown being more effective in decreasing the extracellular titers than the cell-associated viral titers. Pharmacological inhibition of SIRT-1, through EX527 pre-treatment, yielded similar results (Fig. S1A and B). Next, we assessed the effect of SIRT-1 overexpression on EV-D68 titers. Both wild-type (SIRT-1 WT) and the deacetylase inactive mutant (SIRT-1 H363Y) increased EV-D68 extracellular titers (Fig. 1C). Furthermore, overexpression of both wild-type and mutant SIRT-1 constructs partially rescued EV-D68 extracellular titers in SIRT-1 knockdown cells (Fig. S1C), indicating that the pro-EV-D68 activity of SIRT-1 does not require its deacetylase function.

Given SIRT-1's proviral role in EV-D68 infection, we asked whether EV-D68 infection alters SIRT-1 protein levels or subcellular localization. We infected H1HeLa cells for various time points before subjecting the cells to immunofluorescence analysis (IFA) against SIRT-1. As indicated in Fig. 1D, SIRT-1 is localized to the nucleus in the mock-infected cells. EV-D68 infection, on the other hand, induced translocation of a fraction of SIRT-1 to the cytosol (Fig. 1D) beginning at 3hpi, which coincides with peak viral RNA replication. To understand whether SIRT-1 translocation during EV-D68 infection is dependent on exportin-1, the major mammalian nuclear export protein, we pretreated

H1HeLa cells with and without leptomycin-B, a specific exportin-1 inhibitor, followed by EV-D68 infection(Fornerod et al., 1997; Fukuda et al., 1997). Leptomycin-B treatment blocked transcription factor-EB, the master transcriptional regulator of autophagy translocation upon refeeding, as expected (Fig. S2), but it did not obstruct SIRT-1 translocation induced by EV-D68 infection (Fig. S2B). In some cases, cleavage of nuclear pore proteins by picornaviruses has been shown to cause leakage of proteins from the nucleus during infection(Gustin and Sarnow, 2002; Hanson et al., 2019; Watters et al., 2017). However, we found that the autophagy kinase regulator RB1CC1 does not leave the nucleus during EV-D68 infection, indicating that SIRT-1 is being targeted for translocation (Fig S3). We then examined the effect of EV-D68 infection on SIRT-1 protein levels. Results in Fig. 1E and its associated densitometry analysis (Fig. 1F) revealed that in contrast to starvation, which marginally decreased SIRT-1 protein levels, EV-D68 infection does not significantly impact SIRT-1 protein levels.

SIRT-1 promotes autophagy but decreases EV-D68 extracellular titers in autophagy-deficient ATG-7 KO cells

While SIRT-1 is known to regulate autophagy initiation, whether the cellular histone deacetylase is important for basal and stress-induced autophagy is unclear**.** SIRT-1 and scramble knockdown H1HeLa cells were starved or treated with Carbonyl cyanide m-chlorophenylhydrazone (CCCP) to induce or block autophagy, respectively. As shown in Fig. 2A, starvation reduces p62 protein levels, and CCCP treatment increased LC3 lipidation in the scramble control group as expected. In contrast, acute amino acid starvation did not significantly alter p62 protein expression, and CCCP treatment failed

to trigger LC3II accumulation in SIRT-1 knockdown cells, confirming that SIRT-1 is essential for basal and starvation-induced autophagy. To further confirm SIRT-1's importance for basal autophagy, we knocked down SIRT-1 and performed IFA against endogenous LC3.

In contrast to the scramble control, which mainly displayed diffused nuclear-localized LC3, SIRT-1 knockdown provoked endogenous LC3 puncta accumulation near the perinuclear region (Fig. 2B). Similar results were observed in GFP-LC3-overexpressing SIRT-1 knockdown cells, wherein knockdown of SIRT triggered GFP-LC3 puncta accumulation (Fig. S1D). Together, these results confirm that SIRT-1 is essential for stress-induced and basal autophagy.

Given SIRT-1's regulation of autophagy, we asked whether SIRT-1's proviral activity depends on functional autophagy. SIRT-1, which is typically localized to the nucleus in cancer cells, forms a molecular complex with three proteins essential for autophagy initiation: ATG-5, ATG-7, and LC3. SIRT-1 deacetylates these autophagy-related proteins, thereby regulating autophagy induction(Bai and Zhang, 2016; Lee et al., 2008). We first examined whether SIRT-1 colocalizes with ATG-7 during EV-D68 infection. As shown in Fig. 2E, EV-D68 induces ATG-7 puncta formation, which partially colocalizes with SIRT-1. We next examined the effect of ATG-7 knockout (ATG-7 KO), which cannot form autophagosomes, on EV-D68 release. ATG-7 KO severely impeded both extracellular and vesicle-mediated release of EV-D68 (Fig. 2C), consistent with the importance of autophagy for picornavirus release(Jackson, 2014). We then knocked down SIRT-1 in ATG-7 knockout (ATG-7 KO) cells, then infected these cells with EV-D68. Knockdown of SIRT-1 decreased EV-D68 extracellular titers in ATG-7 KO cells

without significantly altering the intracellular titers (Fig. 2D), suggesting that the proviral function of SIRT-1 does not require functional autophagy. Since SIRT-1 regulates autophagy through its deacetylase activity, these data are consistent with our findings in Figure 1.

SIRT-1's proviral activity is mediated by repressing ER stress

SIRT-1 has previously been reported to negatively regulate ER stress by deacetylating X-box binding protein-1 (XBP1)(Wang et al., 2011). To determine whether SIRT-1's proviral activity is mediated via ER stress, we treated H1HeLa cells with or without Thapsigargin (TG), a well-known ER stress inducer, for 5 h after viral adsorption. TG provokes ER stress by inhibiting the Sarco/endoplasmic reticulum Ca2+-ATPase pump (SERCA), which mediates calcium transfer from the cytosol to the lumen of the ER, and is important for maintaining ER homeostasis. While TG treatment only marginally reduced EV-D68 intracellular titers, it markedly decreased the extracellular titers (Fig. 3A), similar to what we observed in SIRT-1 knockdown cells (Fig. 1 A and B). This finding suggests that TG and SIRT-1 may share common cellular targets. To confirm this hypothesis, we treated scramble and SIRT-1 knockdown cells with and without TG after viral adsorption. TG treatment significantly reduced viral extracellular titers in the scramble control group. In contrast, TG did not significantly alter viral extracellular titers when SIRT-1 is depleted (Fig. 3B). We also observed similar results in our genetic epistasis analysis, in which the knockdown of SERCA2A did not further reduce viral titers in SIRT-1-depleted cells (Fig. 3 C and D). We then examined the effect of SIRT-1 depletion and EV-D68 infection on SERCA2A protein levels by western blot. While EV-

D68 infection did not alter SERCA2A levels, the knockdown of SIRT-1 decreases SERCA2A protein levels (Fig. 3E), suggesting SIRT-1 is essential for SERCA2A stability.

Since the induction of ER stress, through either SIRT-1 depletion or TG treatment, attenuates EV-D68 egress, we asked whether EV-D68 infection induces ER stress. For this purpose, H1HeLa cells were mock-infected, infected with EV-D68, or treated with TG for western blot against XBP1, which is upregulated upon ER stress. As expected, TG treatment, which was used as a positive control, induced XBP-1 protein levels in H1HeLa cells (Fig. 3F). In contrast, EV-D68 infection reduced XBP1 levels compared to the mock-infection control (Fig. 3F), indicating that the picornavirus does not trigger ER stress in H1HeLa cells.

Induction of ER stress impairs EV-D68 release in hSABCi-NS1.1 primary cells

To confirm whether TG could impair EV-D68 non-lytic release in a more physiologically relevant cell line, we infected hSABCi-NS1.1 immortalized small airway cells with and without TG. As shown in Fig. 4A, TG treatment significantly reduced EV-D68 extracellular titers without appreciably impacting the intracellular titers, similar to what we observed in H1HeLa cells (Fig. 3A). Our western blot data in Fig. 4B showed that while TG treatment induced BiP protein levels, indicating the induction of ER stress in hSABCi-NS1.1 cells, EV-D68 infection reduced BiP levels compared to the mock control and impaired TG-induced BiP protein expression, suggesting that EV-D68 blocks ER stress. Next, we examined the impact of EX527 pretreatment on EV-D68 titers in the primary cells. Similar to our observation in H1HeLa cells, EX527 reduced EV-D68

extracellular titers and only marginally decreased EV-D68 intracellular titers (Fig. 4C). Finally, we inquired whether EV-D68 infection causes SIRT-1 translocation in these primary cells. As indicated in Fig. 4D, SIRT-1 localizes to the nucleus in uninfected cells. In contrast, EV-D68 infection, as shown by VP3 staining, induces SIRT-1 translocation to the cytosol. These findings demonstrate that SIRT-1's proviral effect in mediating EV-D68 non-lytic release is not cell-type specific.

SIRT-1 Reduces PV, not CVB3, titers

We next sought to understand whether SIRT-1 modulates the infection of other medically important picornaviruses, including PV and CVB3. While protective vaccines are available for PV, few vaccine-derived PV infection cases exist. On the other hand, there is no vaccine or treatment against CVB3, a significant cause of myocarditis and neurological disorders in infants. Therefore, identifying host factors that influence the infection of these viruses could help control their infection. We first examined whether PV and CVB3 alter the subcellular localization of SIRT-1. To our surprise, while PV, similar to EV-D68, induces SIRT-1 translocation to the cytosol, CVB3 did not significantly alter SIRT-1's subcellular localization (Fig. 5A). We then examined the impact of SIRT-1 knockdown on PV and CVB3 infection. SIRT-1 knockdown marginally reduced PV intracellular titers but significantly decreased its extracellular titers (Fig. 5B and 5C). In contrast, the knockdown of SIRT-1 did not alter CVB3 intracellular titers but slightly increased CVB3 extracellular titers (Fig. 5D and 5E). To further confirm SIRT-1's role in PV and CVB3 infection, we pretreated H1HeLa cells with EX527 followed by viral infection. Consistent with siRNA-mediated depletion of SIRT-1, EX527 decreased PV

titers, but not CVB3 titers (Fig. S4). These results indicate that certain but not all picornaviruses require SIRT-1 for their egress from infected cells.

SIRT-1 knockdown reduces the extracellular vesicle-mediated release of enveloped EV-D68 viral particles

Since SIRT-1 knockdown reduces the extracellular EV-D68 titer an order of magnitude more than the intracellular titers, we posit that SIRT-1 proviral activity promotes non-lytic viral release. Multiple members of the *Piconarviridae* family have been previously reported to be released in an enveloped form, usually with multiple virions per vesicle.(Chen et al., 2015; Feng et al., 2013; Robinson et al., 2014; Sin et al., 2017) Hence, we asked whether EV-D68 is similarly released in extracellular vesicles (EVs) and whether SIRT-1 is essential for this process. We knocked down SIRT-1 and isolated EVs for viral titer measurement. As shown in Fig. 6A, EV-D68 appears to be released chiefly in EVs compared to the post-spin supernatant (PSS), and SIRT-1 knockdown severely impeded the extracellular vesicle-mediated release of EV-D68. We knocked down SIRT-1 to understand its impact on viral release. We also examined the expression of CD63, the most widely used marker for exosomes/multivesicular bodies, by western blot. As depicted in Fig. 6B, SIRT-1 knockdown induced CD63 protein levels compared to the scramble control. Given the increase in CD63 protein levels in SIRT-1 knockdown cells, we hypothesize that the knockdown of SIRT-1 may prevent the exocytosis of CD63-positive EVs. To confirm this hypothesis, we infected SIRT-1 knockdown cells for 4 h and isolated the EVs for western blotting against CD63. As shown in Fig. 6C, SIRT-1 knockdown increased CD63 levels in the whole cell lysate.

Our IFA analysis in Fig. 6D also showed the aggregation of sizable CD63-positive puncta in SIRT-1 knockdown cells, as previously observed(Latifkar et al., 2019). Interestingly, for the extracellular vesicle fraction, we observed that SIRT-1 knockdown decreased the release of CD63-positive EVs during EV-D68 infection compared to the scramble control (Fig. 6C). Consistent with the decrease in CD63-positive signal in SIRT-1 knockdown EVs, we detected VP3 only in the scramble control EVs, not EVs purified from SIRT-1 knockdown cells (Fig. 6C). Together, these results indicate that SIRT-1 is essential for EV-D68 release in EVs.

DISCUSSION

Our work shows that SIRT-1, largely thought of as a transcriptional regulator, is essential for the release of the enveloped form of EV-D68. Here, we confirm that SIRT-1 is essential for basal and starvation-mediated autophagy, and traffics to the cytosol during autophagic induction and infeciton. In addition, we show that most EV-D68 is released non-lytically in an enveloped form, and that knockdown or pharmacological inhibition of SIRT-1 severely decreases the release of infectious enveloped EV-D68 particles. Knockdown of SIRT-1 also attenuates the release of PV and SARS-CoV-2 but marginally increases CVB3 egress (Figure 5C,E; Figure 7C). Our results suggest that many viruses induce SIRT-1 translocation to the cytosol to promote their vesicular release. Interestingly, our genetic and pharmacological data lead us to conclude that SIRT-1 is not acting to promote virus release through autophagy, nor through histone deacetylation, but through a mechanism related to ER stress.

We observed that EV-D68 infection induces relocalization of SIRT-1 from the nucleus to the cytosol starting at 3 hpi (Fig. 2B). Given that RNA replication peaks at 3hpi, we initially thought SIRT-1 might be essential for viral RNA replication. However, during EV-D68 infection, SIRT-1 did not colocalize to dsRNA, a marker of active viral RNA replication (Fig. S5A). In contrast, GBF-1, a cellular factor that is required for picornavirus replication, colocalizes with dsRNA during EV-D68 infection (Fig. S5A). The kinetic studies in our supplemental data revealed that starvation induces rapid SIRT-1 translocation to the cytosol as early as 1h post-treatment (Fig. S6A). This finding is consistent with the notion that SIRT-1 drives autophagosome formation during amino acid starvation. Although starvation slightly decreased SIRT-1 protein levels by western blot, pharmacological inhibition of autophagic flux failed to restore SIRT-1 levels. Moreover, SIRT-1 did not colocalize with p62 in starved cells (Fig. S6B), suggesting that the cellular protein is not a substrate for autophagy.

We found that SIRT-1 knockdown did not significantly impact EV-D68 RNA replication (Fig. S5C), virus binding (Fig. S5D), or virus entry (Fig. S5E). Instead, our findings suggest that the effect of SIRT-1 on virus production can largely be explained by a role in re-configuring the exocytosis pathway to promote the release of virus-loaded EVs. Knockdown of SIRT-1 led to the accumulation of large CD63 positive puncta in cells (Fig. 6D), suggesting that the turnover or the release of these vesicles is blocked in the absence of SIRT-1. Infection results in an increase in CD63 in the extracellular vesicles. Interestingly, our western blot data shows a marked decrease in CD63 and a complete lack of VP3 detection in EVs from infected cells with reduced SIRT-1 expression (Fig.

6C). This finding, coupled with the increased CD63 in the whole-cell lysates (Fig. 6B and C), indicates that the reduction of SIRT-1 attenuates the release of virus-loaded CD63-positive EVs.

While picornaviruses are mainly released by cell lysis, a growing body of evidence indicates that these viruses can be released from intact cells without cell lysis, a phenomenon called non-lytic release. For instance, PV has been shown to escape intact cells through AWOL (autophagosome-mediated exit without lysis), in which virus-containing autophagosomes fuse with the plasma membrane to release virions(Jackson et al., 2005; Richards and Jackson, 2012). We show that knockout of ATG-7 reduces EV-D68 extracellular/EV titers, which is consistent with the AWOL model (Fig. 2C and D). Hepatitis A virus (HAV), which is non-lytic, has been reported to exit cells in an enveloped form known as eHAV(Feng et al., 2013; Rivera-Serrano et al., 2019). Similar events, modulated through the autophagic pathway, have been shown for multiple picornaviruses(Chen et al., 2015; Robinson et al., 2014; Sin et al., 2017). We show here for the first time that EV-D68 can also exit intact cells non-lytically in EVs. This extracellular vesicle-mediated release of EV-D68 virions is, as we demonstrate here, dependent upon SIRT-1, a protein best known as a histone deacetylase and autophagy regulator (Fig. 6A). However, our data suggest that SIRT-1's proviral activity is mediated through a role in repressing ER stress.

Studies have shown that SIRT-1 negatively regulates crucial ER stress-related proteins, including XBP1(Wang et al., 2011). Therefore, knocking down SIRT-1 would be

expected to permit ER stress induction, which, in turn, could attenuate EV-D68 non-lytic release. Consistent with this presumption, provoking ER stress through TG treatment, similar to SIRT-1 knockdown, markedly decreases EV-D68 extracellular titers in both H1HeLa and hSABCi cells (Fig. 3A and 4A). Our drug-based epistasis analysis revealed that SIRT-1 and TG share common cellular targets since TG did not further reduce viral titers in SIRT-1 knockdown cells (Fig. 3B).

Since TG binds SERCA2A and blocks its activity leading to ER stress(Lytton et al., 1991), we investigated whether depleting SERCA2A will impact EV-D68 extracellular titers. As anticipated, knocking down SERCA2A reduces EV-D68 release. However, double knockdown of SIRT-1 and SERCA2A failed to appreciably decrease viral titers compared to SERCA2A or SIRT-1 knockdowns alone, indicating SERCA2A is a downstream target of SIRT-1. Intriguingly, we observed that the knockdown of SIRT-1 concomitantly reduced SERCA2A protein levels (Fig. 3E), which is in agreement with a previous study(Gorski et al., 2019). Therefore, knocking down SIRT-1 decreases SERCA2A levels, allowing ER stress induction and decreasing EV-D68 release.

TG has been demonstrated to possess antiviral activity against many viruses using various mechanisms. For instance, TG attenuates Peste des petits ruminants virus (PPRV) and Newcastle disease virus (NDV) infection by restricting viral entry and viral protein synthesis (Kumar et al., 2019). In contrast, TG inhibits respiratory viruses such as Influenza and coronaviruses by provoking a robust interferon response(Al-Beltagi et al., 2021). Here, for the first time, we demonstrate that TG also inhibits EV-

D68 infection (Fig. 3A and 4A). TG's anti-EV-D68 activity seems unlikely to involve blocking viral entry, viral RNA replication, or inducing the type 1 interferon response since the drug treatment only marginally reduced EV-D68 intracellular titers (Fig. 3A and 4A). Instead, TG's anti-EV-D68 activity involves limiting the non-lytic release of EV-D68 (Fig. 3A and 4A).

Although exactly how TG attenuates EV-D68 non-lytic release is unclear, we hypothesize that TG reduces EV-D68 nonlytic release by inducing ER Stress. Consistent with this hypothesis, the knockdown of SERCA2A, which induces ER stress, also reduces EV-D68 release (Fig. 3D). Since EV-D68 infection blocks ER stress, as indicated by the decrease in XBP1 and BiP protein levels, and the lack of BiP induction when EV-D68-infected cells were treated with TG (Fig. 3F and 4B), this suggests that ER stress is detrimental to EV-D68 release. Although we did not observe specific XBP1 or BiP cleavage products during EV-D68 infection, a recent study showed that PV and CVB3 induce cleavage of XBP1 at late time points during their infection(Shishova et al., 2022). However, the study did not determine the specific mechanism of XBP1 cleavage. Nonetheless, decreasing full-length XBP1 and BiP levels during infection may be a common strategy employed by picornaviruses to avoid ER stress, which, as we have shown, is a negative for non-lytic release. While SIRT-1 is thought to negatively regulate Endoplasmic Reticulum stress (ER stress) by deacetylating X-box binding protein-1 (XBP1), we found that the deacetylase inactive mutant (SIRT-1 H363Y) increased EV-D68 release (Fig. 1C). This suggests a non-deacetylase role of SIRT-1 in ER stress, at least during picornavirus infection.

SIRT-1 was previously demonstrated to be essential for MERS-CoV infection(Weston et al., 2019). Here, we demonstrate that the cellular protein is also crucial for SARS-CoV-2 infection. Our data show that, much like in the MERS-CoV study, the knockdown of SIRT-1 decreases SARS-CoV-2 release (Fig. S7C), suggesting that SIRT-1 may be a shared host factor utilized by many Betacoronaviruses.

Our data show that a portion of nuclear SIRT-1 re-localizes to the cytosol upon infection by EV-D68 and PV (Fig. 1D, 4D, and 5A). We also observe that SARS-CoV-2 infection causes SIRT-1 translocation to the cytosol (Fig S7A). These viruses require SIRT-1 for normal virus release. It will be interesting to examine whether other Betacoronaviruses alter the subcellular localization of SIRT-1 and whether SIRT-1 is important for their infection.

CVB3, which does not require SIRT-1, also fails to induce re-localization of the protein (Fig. 5A). This, along with the finding that SIRT-1 is found on virus-induced extracellular vesicles, suggests to us a central role for SIRT-1 in constructing virus-containing vesicles for extracellular release - but only for some viruses. Why at least one picornavirus has evolved a SIRT-1-independent mechanism for release and what the mechanism might be will help understand how to target specific viruses or broad classes of viruses to prevent their release from infected cells. While we believe SIRT-1 is a common regulator of virus release, it is not a universal one. Future work identifying a homolog, or paralog, protein playing a parallel role in CVB3 release, and

understanding the relationship of CVB3 to ER stress, will undoubtedly shed light on the differences between these otherwise similar viruses.

In summary, our data show that SIRT-1 is essential for basal- and stress-induced autophagy and EV-mediated non-lytic release of EV-D68. We also demonstrated that SIRT-1 is crucial for releasing other important public health viruses, including SARS-CoV-2 and PV, indicating that SIRT-1 may be a common host factor regulating multiple viruses' release. Understanding how SIRT-1 regulates viral egress could open avenues for therapeutic intervention against many viruses.

MATERIALS AND METHODS

Cell culture, plasmids, and viruses

H1HeLa cells were purchased from ATCC and cultured in DMEM supplemented with 10% fetal bovine saline, 1x penicillin/streptomycin, and 1x sodium pyruvate. The hSABCi-NS1.1 immortalized small airway cells were grown in PneumaCult™-Ex Plus Basal Medium supplemented with PneumaCult™-Ex Plus 50x supplement, 0.2x Hydrocortisone, 1x penicillin/streptomycin,1.25µg/mL Amphotericin B, and 0.5mg/mL Gentamycin. The cells were incubated at 37°C in a 5% CO_2 incubator. The wild-type (Flag-SIRT1) and mutant (Flag-SIRT1 H363Y) SIRT-1 plasmids were purchased from Addgene and transfected into cells using lipofectamine 2000. The transfection complex was replaced with basal media 6 h post-transfection.

All work with SARS-CoV-2 was performed in a BSL3 laboratory and approved by our Institutional Biosafety Committee (IBC#00005484). Vero E6 cells overexpressing transmembrane serine protease 2 (TMPRSS2) (VeroT) (ATCC CRL 1586) were cultured in DMEM medium (Quality Biological) supplemented with 10% (vol/vol) heat-inactivated FBS (Sigma), 1% (vol/vol) penicillin-streptomycin (Gemini Bio-Products) and 1% (vol/vol) l-glutamine (2 mM final concentration; Gibco). A549 cells overexpressing human angiotensin-converting enzyme 2 (hACE2, A549/hACE2) were generously provided by Dr. Brad Rosenberg (Daniloski et al., 2021). They were cultured in DMEM medium (Quality Biological) supplemented with 10% (vol/vol) heat-inactivated FBS (Sigma), and 1% (vol/vol) penicillin-streptomycin (Gemini Bio-Products). For induction of autophagy by starvation before infection, cells were starved for 4 h with the “Axe” media (an amino acid deficient media that is widely used to induce autophagic flux)(Axe et al., 2008).

Western blot

Cells were lysed using RIPA buffer supplemented with cOmplete Tablets Mini Protease Inhibitor Cocktail. The lysates were incubated on ice for at least 30 minutes before being clarified at 12000 rpm for 30 minutes. The supernatants were transferred into Eppendorf tubes, and protein concentrations were determined by Bradford assay. Lysates were then boiled and loaded onto SDS-PAGE. Following transfer onto PVDF membranes, the membranes were blocked in 5% skim milk for 1 h, washed twice with TBST, and stained with the following primary antibodies: anti-SQSTM1/p62, anti-LC, anti-β-actin at 1: 1000 dilutions, anti-CD63 (1: 250), anti-SERCA2A (1: 500) and anti-

XBP1 (1: 500) overnight. The membranes were stained with the secondary antibodies for 1 h at room temperature and imaged using the Chemidoc machine after two washes.

Immunofluorescence analysis (IFA)

The cells were fixed with 4% paraformaldehyde at room temperature for 20 minutes and then permeabilized with 0.3% Triton-X for 30 minutes. The cells were blocked with 3% BSA for 1 h on a shaker and incubated with primary antibodies at 1: 250 dilutions overnight at 4°C. The cells were washed twice with PBS, incubated with the secondary antibodies (1:250), rewashed three times, and imaged with an ECHO Revolve fluorescence microscope.

Extracellular vesicle isolation

Extracellular vesicles were isolated using the Invitrogen Total Exosome Isolation Reagent (from cultured cells). In brief, 1 ml of cell culture supernatants were clarified at 2000 x g for 30 minutes. The supernatants were then transferred to Eppendorf tubes, and 500 µl of the exosome isolation buffer was added and incubated at 4°C overnight. At the end of the incubation, the tubes were centrifuged for 1 h at 10000 x g. The supernatants were transferred to new Eppendorf tubes, and the pellets were resuspended in PBS for western blot or plaque assay.

RNA isolation and qPCR

TRIzol was used to isolate total RNA according to the manufacturer's instructions, and cDNA was synthesized using the Thermo Scientific RevertAid H Minus First Strand

cDNA Synthesis Kit. KiCqStart SYBR qPCR Ready Mix was used to perform qPCR using the Fast Dx Real-Time PCR Instrument (Applied Biosystems). Primers specific to the 5′ untranslated region (5′ TAACCCGTGTGTAGCTTGG-3′ and 5′ -ATTAGCCGCATTCAGGGGC-3′) were used to amplify EV-D68, and gene expression was normalized to GAPDH and plotted as relative expression compared to the 0h infection-only time point.

Plaque assay

The cells were washed twice with PBS for cell-associated titer determination and scraped in 1ml PBS, after which they were subjected to three freeze-thaw cycles and added to H1HeLa cells for 30 minutes. Cells were then overlaid with a 1:1 ratio of 2x MEM and 2% agar for 48 h before staining plaques with crystal violet. For extracellular titers, 1 ml of supernatants were collected and treated as the cell-associated titer without being subjected to free-thaw cycles.

siRNA transfections

siRNAs were transfected into cells using lipofectamine as previously described. In brief, 200 nM of siRNA and 10 µl of Lipofectamine 2000 were separately incubated in Opti-MEM at room temperature for 5 minutes. The siRNAs and lipofectamine were mixed and incubated for 20 minutes before being added to cells that were 40% confluent. The transfection complexes were replaced with growth media at 6 h post-transfection. The cells were then used for viral infection or western blot for transfection efficiency determination.

Virus entry assays

Scramble and SIRT-1 knockdown cells were pre-chilled on ice for 30 minutes for viral binding assay. The cells were then infected with EV-D68 (MOI =30) for 1 h on ice. The inoculum was removed, and the cells were washed twice with PBS, scraped, freeze-thawed 3 times, and stored at -80°C for plaque assay.

For viral entry, scramble and SIRT-1 knockdown cells were similarly pre-chilled on ice for 30 minutes and then infected with EV-D68 for 30 minutes on ice. The unbound viral particles were washed off with PBS before shifting the cells to 37°C, allowing viral entry for 1 h. The cells were finally washed with PBS, scraped into Eppendorf tubes, and prepared for plaque assay.

SARS-CoV-2 titer determination by plaque assay

Plaque assays were performed as described previously (Coleman and Frieman, 2015). Briefly, 12-well plates were seeded with 2 x 10^5 VeroT cells/well one day before processing. On the day of processing, media was removed from the 12-well plates, and 200 µl of dilutions of virus stock or collected cell supernatants in DMEM were added to each well. Plates were incubated at 37°C (5% CO^2) for 1 hour with rocking every 15 minutes. Following incubation, 2 ml of plaque assay media, DMEM containing 0.1% agarose (UltraPure™) and 2% FBS (Gibco), was added to each well and incubated for 48 h at 37°C (5% CO^2). Following incubation, plates were fixed with 4% paraformaldehyde, stained with 0.25% crystal violet (w/v), plaques counted, and titers calculated as plaque-forming units (PFU)/ml.

siRNA Knockdown Protocol for SARS-CoV-2 infection

siRNA knockdown assays were performed as described previously (Weston et al., 2020). Briefly, A549/hACE2 cells were seeded in 24-well cell culture plates one day before siRNA treatment. On the day of treatment, 4.4 µl Opti-MEM (Gibco) and 2.2 µl Oligofectamine (Thermo Scientific) were combined and incubated for 5 minutes at room temperature. This mixture was then added to 35.5 µl Opti-MEM and 0.8µl of 50 µM siRNA and incubated for 20 minutes at room temperature. Following incubation, a further 177 µl of Opti-MEM was added to the transfection mixture, media were removed from cells, and 200 µl of transfection mixture was added. After a 4 h incubation at 37°C/5% CO^2, 200 µl of DMEM (+20% FBS) was added to the cells resulting in a final concentration of 10% FBS. Cells were then incubated at 37°C/5% CO^2 overnight. Following incubation, cells were infected with SARS-CoV-2 (WA1, MOI = 0.01 for titer, MOI = 0.5 for IFA), and supernatants were collected 24 hours post-infection. SARS-CoV-2 titers from supernatants were determined by plaque assay.

Statistical analysis

GraphPad Prism software (Version 7.03) was used for all statistical analyses, and values represent the mean ± standard error of the mean (SEM) of at least 3 independent repeats. Student t-test was used for comparison and a p-value of < 0.05. was considered statistically significant.

ACKNOWLEDGEMENTS

We thank Sohha Ariannejad for assistance and the members of the Jackson, Frieman, and Coughlan labs for thoughtful discussion. This work was funded by NIH/NIAID grants R01141359, R01104928 to W.T.J. and R21158134 to W.T.J. and M.B.F.

FIGURE LEGENDS

Figure 1. EV-D68 infection changes SIRT-1's subcellular localization. H1HeLa cells were transfected with either scramble control or SIRT-1 siRNAs for 48 h. The cells were then infected with EV-D68 (MOI = 0.1) for 5 h. The intracellular (A) and extracellular (B) particles were collected for plaque assay. (C) Cells were transfected with the indicated plasmids for 24 h before being infected with EV-D68 (MOI = 0.1) for 5 h. The extracellular particles were collected and analyzed by a plaque assay. (D) H1HeLa cells were infected for the indicated time points for IFA analysis against SIRT-1. (E) H1HeLa cells were infected (MOI = 30) for 4 h. Lysates were collected for western blot against SIRT-1. (F) Densitometry quantitation of E.. Error bars denote the mean ± SEM of 3 independent repeats. Unpaired student's t-test was used for the statistical analyses (**= $p < 0.01$;* = $p \leq 0.05$; ns=not significant.) Scale bar = 6.2 μm.

Figure 2. SIRT-1 promotes autophagy but decreases EV-D68 extracellular titers in autophagy-deficient ATG-7 KO cells. (A) H1HeLa cells were transfected with scramble or SIRT-1 siRNA for 48 h. The cells were subsequently starved or treated with CCCP (10 μM) for 4 h. Lysates were harvested and analyzed by western blot. (B) Cells were transfected with the indicated siRNAs for 48 h before being fixed and subjected to

IFA against endogenous LC3. (C) H1HeLa and ATG-7 KO cells were infected with 0.1 MOI of EV-D68 for 5h. The extracellular vesicles were isolated as described in the materials and methods and viral titers were determined by a plaque assay. (D) ATG-7 KO cells were transfected with scramble or SIRT-1 siRNAs for 48 h and infected as in C, followed by plaque assay-based viral titer determination. (E) H1Hela cells were infected with EV-D68 (MOI =30) for 4 h. The cells were fixed and immuno-stained with antibodies against SIRT-1 and ATG-7. Error bars denote the mean ± SEM of 3 independent repeats. Unpaired student's t-test was used for the statistical analyzes (***= p< 0.001; ns=not significant.) Scale bar = 6 µm.

Figure 3. The proviral activity of SIRT-1 is mediated through ER stress. (A) H1HeLa cells were infected with EV-D68 (MOI =0.1) for 30 minutes. The cells were washed and replenished with complete media with or without 2 µM TG for 5 h. Viral titers were determined by plaque assay. (B) Cells were transfected with either scramble control siRNA or SIRT-1 siRNA for 48 h. The cells were infected and treated as in A, and viral extracellular titers were similarly measured by plaque assay. (C and D) Cells were transfected with the indicated siRNAs for 48 h for western blot (C) or viral titer determination (D) following EV-D68 infection (MOI =0.1) for 5 h. (E) H1HeLa cells were transfected for 48 h with the indicated siRNAs, and either mock-infected or infected (

with EV-D68 MOI =30) for 4 h. Lysates were collected, and a western blot was performed against the indicated proteins. (F) H1HeLa cells were mock-infected, treated with TG for 4 h, or infected with EV-D68 (MOI =30) for 4 h for western blot against XBP1. Error bars indicate mean ± SEM. Unpaired student's t-test was used for the statistical analysis (***= $p < 0.001$; **= $p < 0.01$;* = $p \leq 0.05$; ns=not significant.)

Figure 4. Induction of ER stress impairs EV-D68 release in hSABCi-NS1.1 cells. (A) hSABCi-NS1.1 cells were infected with 0.1 MOI of EV-D68 for 30 mins. The cells were washed and replenished with basal media or media containing 2 μM TG for 6 h. Viral titers were determined by plaque assay. (B) hSABCi-NS1.1 cells were mock-infected, infected with EV-D68, and treated with or without TG for 6 h, or treated with TG alone for 6 h. The lysates were harvested and a western blot was performed against the indicated proteins. (C) hSABCi-NS1.1 were pretreated with 50 μM EX527 for 48 h. The cells were then infected with EV-D68 (MOI=0.1) for 6 h for a plaque assay. (D) hSABCi-NS1.1 cells were mock-infected or infected with EV-D68 (MOI =30) for 6 h. The

cells were fixed for IFA against endogenous SIRT-1. Error bars represent mean ± SEM. (** = $p < 0.01$; * = $p \leq 0.05$; ns = not significant.). Scale bar = 7.5 µm.

Figure 5. SIRT-1 is critical for PV, but not CVB3, release from cells. (A) H1HeLa cells were mock-infected or infected with PV or CVB 3 for 4 h. The cells were fixed, and IFA was done against SIRT-1 MOI = 30. (B and C) Cells were transfected with scramble or SIRT-1 siRNAs for 48 h before being infected with PV (MOI = 0.1) for 5 h. Viral titers were determined by a plaque assay. (D and E) Cells were transfected and infected with CVB3 as in B. n = 3 independent experiments, and error bars represent mean ± SEM. (*** = $p < 0.001$; * = $p \leq 0.05$; ns = not significant.). Scale bar = 7.5 µm.

Figure 6. SIRT-1 KD reduces Extracellular vesicle-mediated release of infectious EV-D68 viral particles. H1HeLa cells were transfected with SIRT-1 and Scramble siRNAs for 48 h. (A) Cells were infected with EV-D68 (MOI = 0.1) for 5 h, and EVs were isolated for viral titer measurement by plaque assay. (B) Cells were transfected as in A, and the whole-cell lysates (WCL) were collected and prepared for western blot against CD63. (C) H1HeLa cells were transfected with the indicated siRNAs for 48 h. The cells

were either left uninfected or infected with MOI 30 of EV-D68 for 4 h. The EVs and WCL were prepared for western blot against the indicated proteins. (D) Cells were plated on cover slides and transfected with scramble or SIRT-1 siRNA for 48 h. The cells were then fixed and subjected to immunofluorescence analysis against CD63. Arrows indicate large CD63 puncta. Error bars indicate mean ± SEM. Unpaired student's t-test was used for the statistical analysis (**= $p < 0.01$;* = $p \leq 0.05$.) Scale bar = 6.5 µm.

Supplemental Figure 1. SIRT-1 in LC3 puncta formation and virus release. H1HeLa cells were pretreated with 50 µM EX527 for 24 h, followed by 0.1 MOI EV-D68 infection. The intracellular (B) and extracellular (C) viral titers were determined by a plaque assay. (C) H1HeLa cells were transfected with scramble control or SIRT-1 siRNA for 24 h, after which the cells were reseeded and transfected with the DNA constructs for 24 h. The cells were then infected with EV-D68 (MOI =0.1) for 5 h. A plaque assay was used to determine the viral titer. (D) H1HeLa cells were transfected with either scramble or SIRT-1 siRNA for 48 h. GFP-LC3 transfection was initiated at 24 h post-siRNA transfection for 24 h. The cells were then fixed, and images were acquired with a revolve microscope. (** = $p < 0.01$; * = $p \leq 0.05$; ns = not significant.).

Supplemental Figure 2. LMB blocks TFEB nuclear export but not SIRT-1 translocation during EV-D68 infection. (A) Cells were left untreated, starved, starved and then refeed with complete media for 1 h, or starved and refeed with complete media containing 10 nM leptomycin B for 1 h. The cells were fixed, and IFA was performed against endogenous TFEB. (B) Cells were pretreated with 50 nM of LMB for 2 h. The cells were then infected (MOI =30) for 30 minutes (adsorption) and incubated with and without LMB until the end of the infection (4h) for IFA against SIRT-1. Starvation for 4 h was included as a control.

Supplemental Figure 3. EV-D68 infection does not alter RB1CC1 subcellular localization. H1HeLa cells were mock-infected or infected with EV-D68 at an MOI of 30 for 4 h, before subjecting the cells to IFA against RB1CC1.

Supplemental Figure 4. EX527 pretreatment reduced PV, but not CVB3 titers. H1HeLa cells pretreated with EX527 (50 µM) for 24 h were infected with PV and CVB3 (MOI = 0.1) for 5h. The intracellular and extracellular titers for PV (A and B) and for CVB3 (C and D) were determined by a plaque assay. (** = $p < 0.01$; ns = not significant.).

Supplemental Figure 5. SIRT-1 is not required for EV-D68 entry and replication. (A) Cells were infected for the indicated time point, fixed, and processed for IFA against

SIRT-1 and dsRNA. (B) Cells were infected as in A for IFA against GBF-1, and dsRNA (C) H1HeLa cells were transfected with scramble or SIRT-1 siRNA for 48 h. The cells were then infected (MOI = 0.1) for the indicated time point for the qPCR assay. (D and E) Cells were transfected as in B, and virus binding and entry assays were performed as described in the materials and methods. (ns = non significant). Scale bar = 6.2 µm.

Supplemental Figure 6. SIRT-1 does not colocalize with p62 during starvation. (A) H1HeLa cells were starved for the indicated periods, fixed, and subjected to IFA against SIRT-1. (B) H1HeLa cells were treated with and without the Axe starvation media for 2 h. The cells were then fixed and immunostained using antibodies against SIRT-1 and p62.

Supplemental Figure 7. SARS-CoV-2 infection requires SIRT-1 and induces SIRT-1 translocation to the cytosol. (A) A549-ACE2 cells were infected with SAR-CoV-2 (MOI = 0.5) for 24 h. The cells were fixed and subjected to IFA against SIRT-1 and SARS-CoV-2 nucleoprotein. (B) A549-ACE2 cells were transfected with SIRT-1 siRNA for 48 h. Lysates were analyzed by western blot. (C) Cells were transfected as in B and infected (MOI 0.01) for 48 h before being subjected to a plaque assay for viral titer measurement. (** = $p < 0.01$). Scale bar = 30 µm.

REFERENCES

Ahmad L, Mostowy S, Sancho-Shimizu V. 2018. Autophagy-Virus Interplay: From Cell Biology to Human Disease. *Front Cell Dev Biol* **6**:155.

Al-Beltagi S, Preda CA, Goulding LV, James J, Pu J, Skinner P, Jiang Z, Wang BL, Yang J, Banyard AC, Mellits KH, Gershkovich P, Hayes CJ, Nguyen-Van-Tam J, Brown IH, Liu J, Chang K-C. 2021. Thapsigargin Is a Broad-Spectrum Inhibitor of Major Human Respiratory Viruses: Coronavirus, Respiratory Syncytial Virus and Influenza A Virus. *Viruses* **13**. doi:10.3390/v13020234

Axe EL, Walker SA, Manifava M, Chandra P, Roderick HL, Habermann A, Griffiths G, Ktistakis NT. 2008. Autophagosome formation from membrane compartments enriched in phosphatidylinositol 3-phosphate and dynamically connected to the endoplasmic reticulum. *J Cell Biol* **182**:685–701.

Bai W, Zhang X. 2016. Nucleus or cytoplasm? The mysterious case of SIRT1's subcellular localization. *Cell Cycle*.

Chalkiadaki A, Guarente L. 2015. The multifaceted functions of sirtuins in cancer. *Nat Rev Cancer* **15**:608–624.

Chen Y-H, Du W, Hagemeijer MC, Takvorian PM, Pau C, Cali A, Brantner CA, Stempinski ES, Connelly PS, Ma H-C, Jiang P, Wimmer E, Altan-Bonnet G, Altan-Bonnet N. 2015. Phosphatidylserine vesicles enable efficient en bloc transmission of enteroviruses. *Cell* **160**:619–630.

Coleman CM, Frieman MB. 2015. Growth and Quantification of MERS-CoV Infection. *Curr Protoc Microbiol* **37**:15E.2.1–9.

Daniloski Z, Jordan TX, Wessels H-H, Hoagland DA, Kasela S, Legut M, Maniatis S, Mimitou EP, Lu L, Geller E, Danziger O, Rosenberg BR, Phatnani H, Smibert P, Lappalainen T, tenOever BR, Sanjana NE. 2021. Identification of Required Host Factors for SARS-CoV-2 Infection in Human Cells. *Cell* **184**:92–105.e16.

Eshaghi A, Duvvuri VR, Isabel S, Banh P, Li A, Peci A, Patel SN, Gubbay JB. 2017. Global Distribution and Evolutionary History of Enterovirus D68, with Emphasis on the 2014 Outbreak in Ontario, Canada. *Front Microbiol* **8**:257.

Esposito S, Bosis S, Niesters H, Principi N. 2015. Enterovirus D68 Infection. *Viruses* **7**:6043–6050.

Feng Z, Hensley L, McKnight KL, Hu F, Madden V, Ping L, Jeong S-H, Walker C, Lanford RE, Lemon SM. 2013. A pathogenic picornavirus acquires an envelope by hijacking cellular membranes. *Nature* **496**:367–371.

Fornerod M, Ohno M, Yoshida M, Mattaj IW. 1997. CRM1 is an export receptor for leucine-rich nuclear export signals. *Cell* **90**:1051–1060.

Fukuda M, Asano S, Nakamura T, Adachi M, Yoshida M, Yanagida M, Nishida E. 1997. CRM1 is responsible for intracellular transport mediated by the nuclear export signal. *Nature* **390**:308–311.

Gorski PA, Jang SP, Jeong D, Lee A, Lee P, Oh JG, Chepurko V, Yang DK, Kwak TH, Eom SH, Park Z-Y, Yoo YJ, Kim DH, Kook H, Sunagawa Y, Morimoto T, Hasegawa K, Sadoshima J, Vangheluwe P, Hajjar RJ, Park WJ, Kho C. 2019. Role of SIRT1 in Modulating Acetylation of the Sarco-Endoplasmic Reticulum Ca2+-ATPase in Heart Failure. *Circ Res* **124**:e63–e80.

Green DR, Levine B. 2014. To Be or Not to Be? How Selective Autophagy and Cell Death Govern Cell Fate. *Cell* **157**:65–75.

Gustin KE, Sarnow P. 2002. Inhibition of nuclear import and alteration of nuclear pore complex composition by rhinovirus. *J Virol* **76**:8787–8796.

Hanson PJ, Hossain AR, Qiu Y, Zhang HM, Zhao G, Li C, Lin V, Sulaimon S, Vlok M, Fung G,

Chen VH, Jan E, McManus BM, Granville DJ, Yang D. 2019. Cleavage and Sub-Cellular Redistribution of Nuclear Pore Protein 98 by Coxsackievirus B3 Protease 2A Impairs Cardioprotection. *Front Cell Infect Microbiol* **9**:265.

Hetz C. 2012. The unfolded protein response: controlling cell fate decisions under ER stress and beyond. *Nat Rev Mol Cell Biol* **13**:89–102.

Huang R, Xu Y, Wan W, Shou X, Qian J, You Z, Liu B, Chang C, Zhou T, Lippincott-Schwartz J, Liu W. 2015. Deacetylation of nuclear LC3 drives autophagy initiation under starvation. *Mol Cell* **57**:456–466.

Jackson WT. 2014. Poliovirus-induced changes in cellular membranes throughout infection. *Curr Opin Virol* **9**:67–73.

Jackson WT, Giddings TH Jr, Taylor MP, Mulinyawe S, Rabinovitch M, Kopito RR, Kirkegaard K. 2005. Subversion of cellular autophagosomal machinery by RNA viruses. *PLoS Biol* **3**:e156.

Jing H, Lin H. 2015. Sirtuins in epigenetic regulation. *Chem Rev* **115**:2350–2375.

Koga T, Suico MA, Shimasaki S, Watanabe E, Kai Y, Koyama K, Omachi K, Morino-Koga S, Sato T, Shuto T, Mori K, Hino S, Nakao M, Kai H. 2015. Endoplasmic Reticulum (ER) Stress Induces Sirtuin 1 (SIRT1) Expression via the PI3K-Akt-GSK3β Signaling Pathway and Promotes Hepatocellular Injury. *J Biol Chem* **290**:30366–30374.

Kumar N, Khandelwal N, Kumar R, Chander Y, Rawat KD, Chaubey KK, Sharma S, Singh SV, Riyesh T, Tripathi BN, Barua S. 2019. Inhibitor of Sarco/Endoplasmic Reticulum Calcium-ATPase Impairs Multiple Steps of Paramyxovirus Replication. *Front Microbiol* **10**:209.

Lang M, Mirand A, Savy N, Henquell C, Maridet S, Perignon R, Labbe A, Peigue-Lafeuille H. 2014. Acute flaccid paralysis following enterovirus D68 associated pneumonia, France, 2014. *Euro Surveill* **19**. doi:10.2807/1560-7917.es2014.19.44.20952

Latifkar A, Ling L, Hingorani A, Johansen E, Clement A, Zhang X, Hartman J, Fischbach C, Lin H, Cerione RA, Antonyak MA. 2019. Loss of Sirtuin 1 Alters the Secretome of Breast Cancer Cells by Impairing Lysosomal Integrity. *Dev Cell* **49**:393–408.e7.

Lee IH, Cao L, Mostoslavsky R, Lombard DB, Liu J, Bruns NE, Tsokos M, Alt FW, Finkel T. 2008. A role for the NAD-dependent deacetylase Sirt1 in the regulation of autophagy. *Proc Natl Acad Sci U S A* **105**:3374–3379.

Li X, Zhang K-Y, Zhang P, Chen L-X, Wang L, Xie M, Wang C-Y, Tang X-Q. 2014. Hydrogen sulfide inhibits formaldehyde-induced endoplasmic reticulum stress in PC12 cells by upregulation of SIRT-1. *PLoS One* **9**:e89856.

Lytton J, Westlin M, Hanley MR. 1991. Thapsigargin inhibits the sarcoplasmic or endoplasmic reticulum Ca-ATPase family of calcium pumps. *J Biol Chem* **266**:17067–17071.

Oslowski CM, Urano F. 2011. Measuring ER stress and the unfolded protein response using mammalian tissue culture system. *Methods Enzymol* **490**:71–92.

Richards AL, Jackson WT. 2012. Intracellular vesicle acidification promotes maturation of infectious poliovirus particles. *PLoS Pathog* **8**:e1003046.

Rivera-Serrano EE, González-López O, Das A, Lemon SM. 2019. Cellular entry and uncoating of naked and quasi-enveloped human hepatoviruses. *Elife* **8**. doi:10.7554/eLife.43983

Robinson SM, Tsueng G, Sin J, Mangale V, Rahawi S, McIntyre LL, Williams W, Kha N, Cruz C, Hancock BM, Nguyen DP, Sayen MR, Hilton BJ, Doran KS, Segall AM, Wolkowicz R, Cornell CT, Whitton JL, Gottlieb RA, Feuer R. 2014. Coxsackievirus B exits the host cell in shed microvesicles displaying autophagosomal markers. *PLoS Pathog* **10**:e1004045.

Shi J, Luo H. 2012. Interplay between the cellular autophagy machinery and positive-stranded RNA viruses. *Acta Biochim Biophys Sin* **44**:375–384.

Shishova A, Dyugay I, Fominykh K, Baryshnikova V, Dereventsova A, Turchenko Y, Slavokhotova AA, Ivin Y, Dmitriev SE, Gmyl A. 2022. Enteroviruses Manipulate the Unfolded Protein Response through Multifaceted Deregulation of the Ire1-Xbp1 Pathway. *Viruses* **14**. doi:10.3390/v14112486

Singh P, Reza MI, Syed AA, Garg R, Husain A, Katekar R, Goand UK, Riyazuddin M, Gupta AP, Gayen JR. 2020. PSTi8 with metformin ameliorates perimenopause induced steatohepatitis associated ER stress by regulating SIRT-1/SREBP-1c axis. *Heliyon* **6**:e05826.

Sin J, McIntyre L, Stotland A, Feuer R, Gottlieb RA. 2017. Coxsackievirus B escapes the infected cell in ejected mitophagosomes. *J Virol* **91**. doi:10.1128/JVI.01347-17

Tang Y-Y, Wang A-P, Wei H-J, Li M-H, Zou W, Li X, Wang C-Y, Zhang P, Tang X-Q. 2018. Role of silent information regulator 1 in the protective effect of hydrogen sulfide on homocysteine-induced cognitive dysfunction: Involving reduction of hippocampal ER stress. *Behav Brain Res* **342**:35–42.

Wang F-M, Chen Y-J, Ouyang H-J. 2011. Regulation of unfolded protein response modulator XBP1s by acetylation and deacetylation. *Biochem J* **433**:245–252.

Watters K, Inankur B, Gardiner JC, Warrick J, Sherer NM, Yin J, Palmenberg AC. 2017. Differential Disruption of Nucleocytoplasmic Trafficking Pathways by Rhinovirus 2A Proteases. *J Virol* **91**. doi:10.1128/JVI.02472-16

Weston S, Baracco L, Keller C, Matthews K, McGrath ME, Logue J, Liang J, Dyall J, Holbrook MR, Hensley LE, Jahrling PB, Yu W, MacKerell AD Jr, Frieman MB. 2020. The SKI complex is a broad-spectrum, host-directed antiviral drug target for coronaviruses, influenza, and filoviruses. *Proc Natl Acad Sci U S A* **117**:30687–30698.

Weston S, Matthews KL, Lent R, Vlk A, Haupt R, Kingsbury T, Frieman MB. 2019. A Yeast Suppressor Screen Used To Identify Mammalian SIRT1 as a Proviral Factor for Middle East Respiratory Syndrome Coronavirus Replication. *J Virol* **93**. doi:10.1128/JVI.00197-19

Yoshida H, Matsui T, Yamamoto A, Okada T, Mori K. 2001. XBP1 mRNA is induced by ATF6 and spliced by IRE1 in response to ER stress to produce a highly active transcription factor. *Cell* **107**:881–891.

Fig. 1 EV-D68 infection changes SIRT-1's subcellular localization

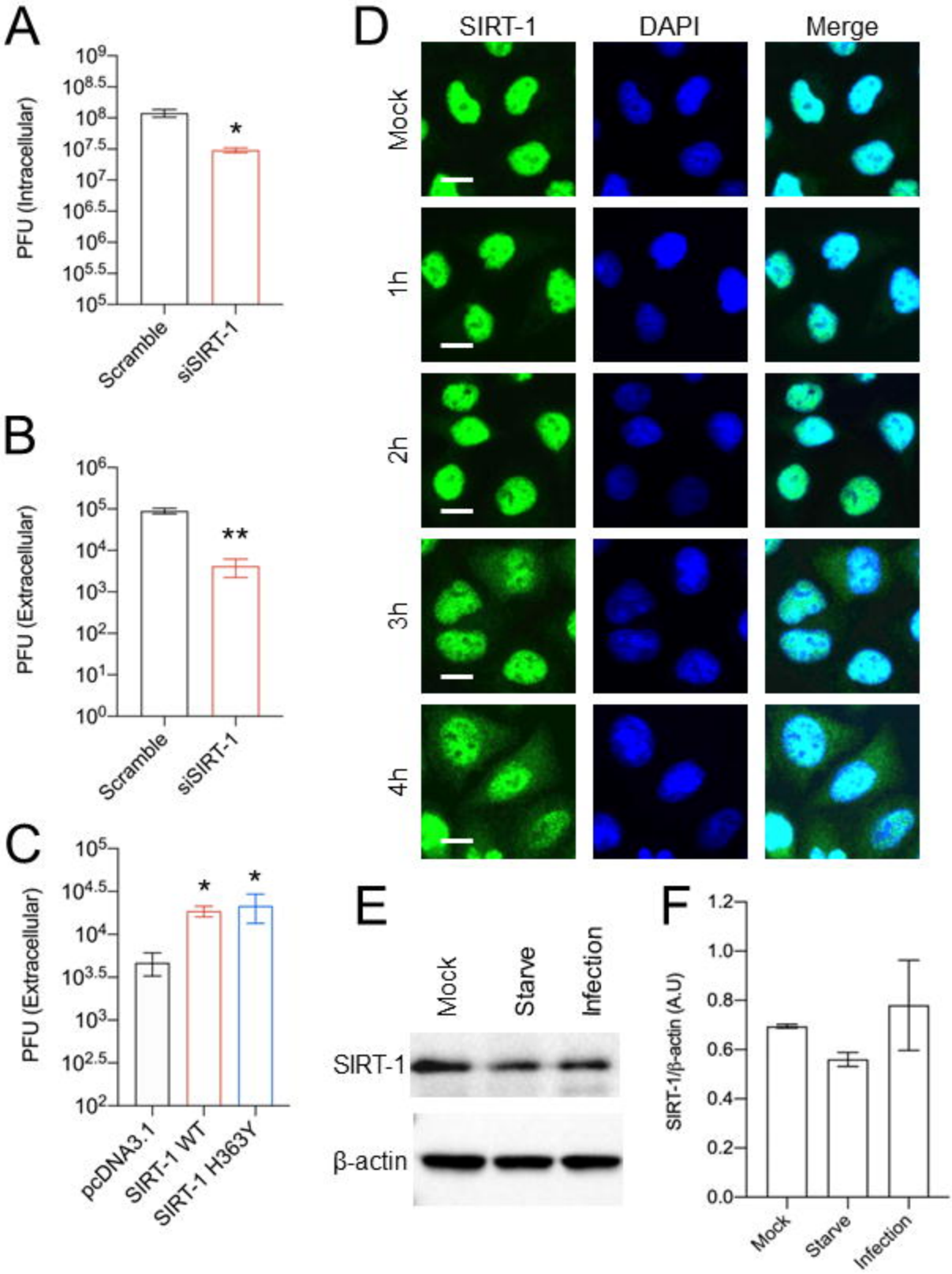

Fig. 2 SIRT-1 promotes autophagy, but decreases EV-D68 extracellular titers in autophagy deficient ATG-7 KO cells

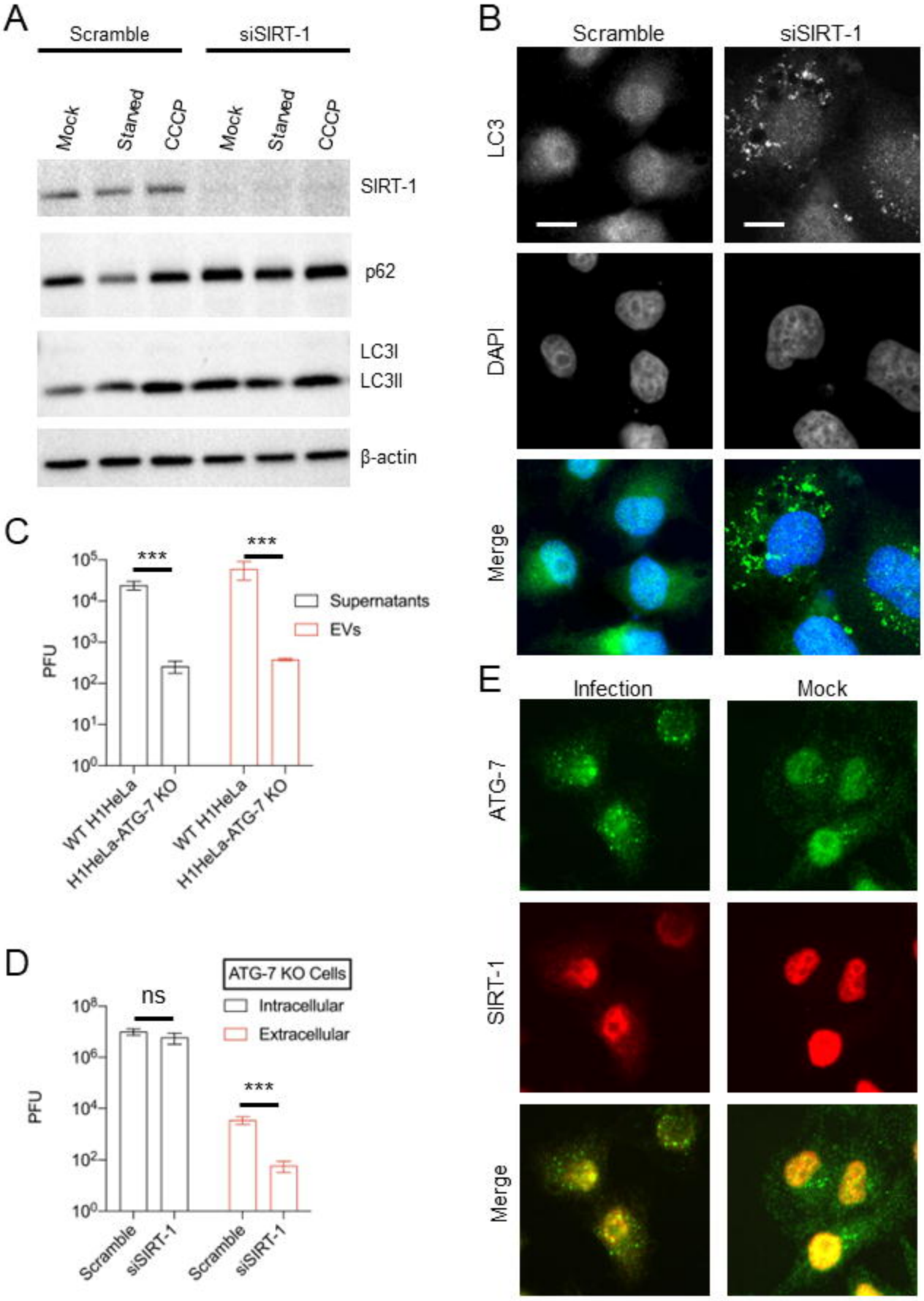

Fig. 3 The proviral activity of SIRT-1 is mediated through ER stress

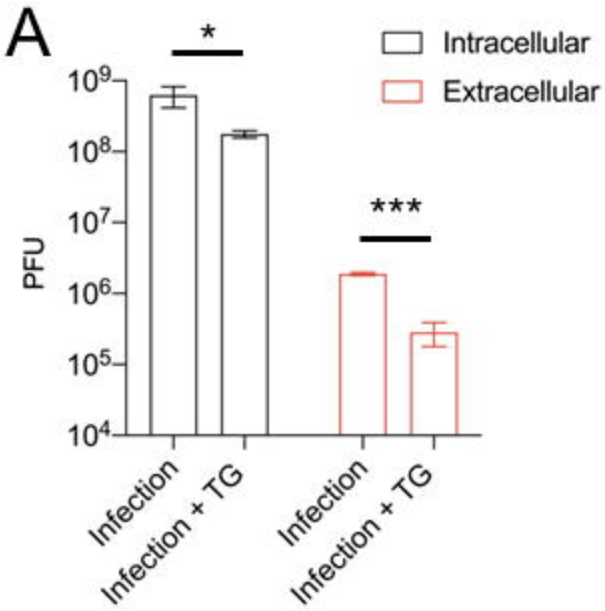

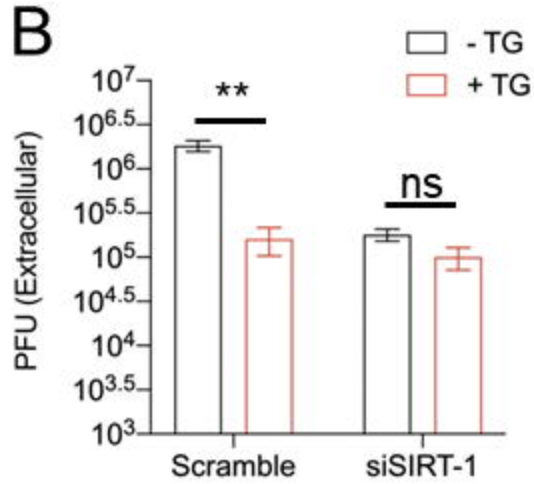

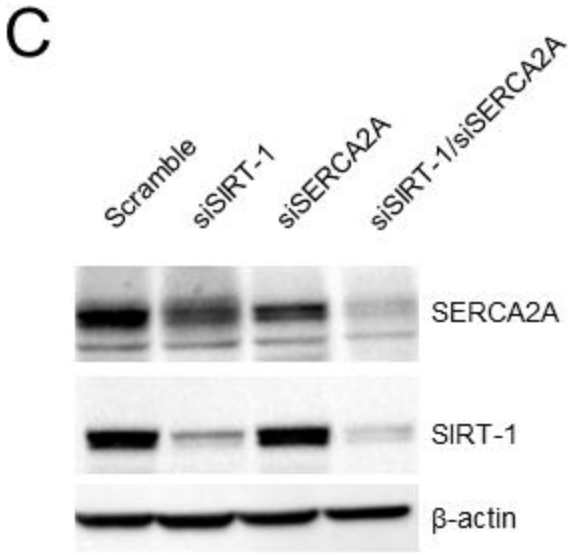

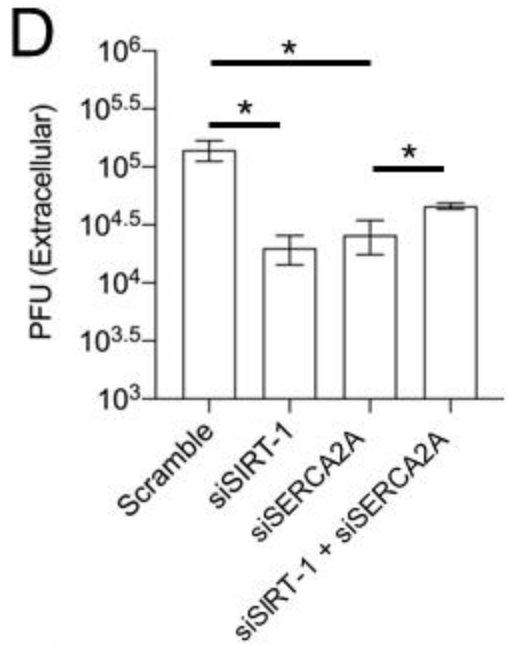

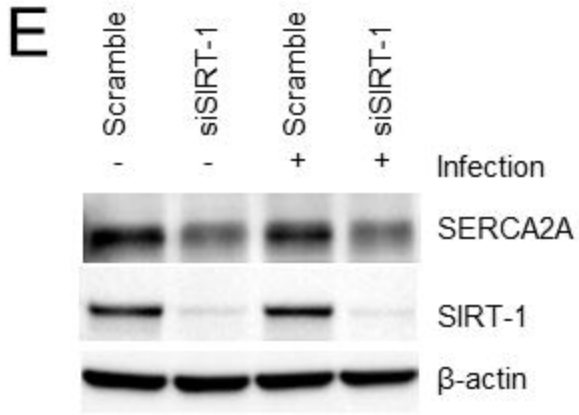

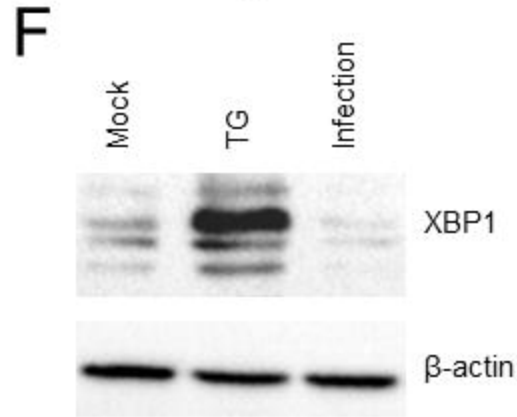

Fig. 4 Induction of ER stress impairs EV-D68 release in hSABCi cells

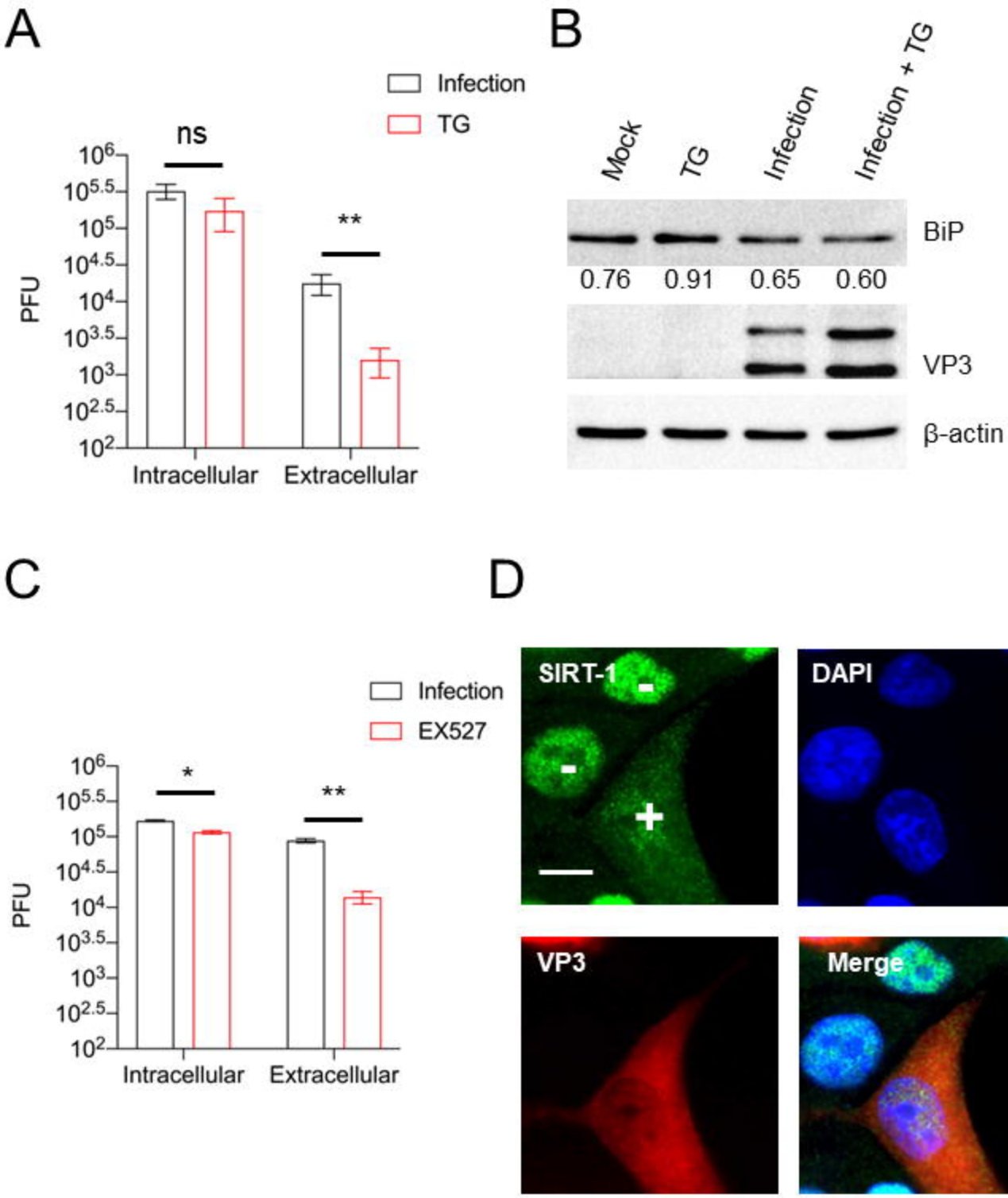

Fig. 5 SIRT-1 is critical for PV, but not CVB3, release from cells

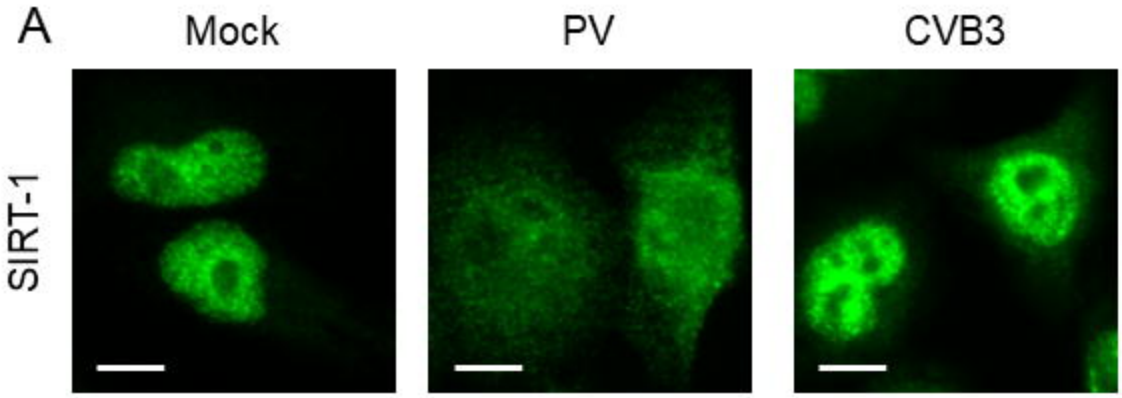

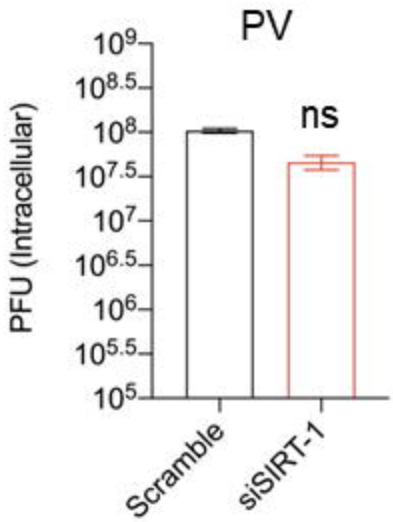

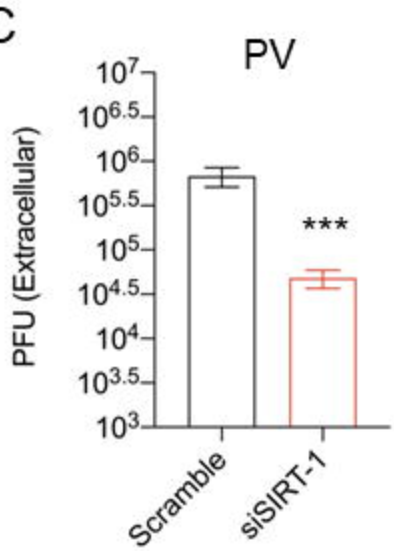

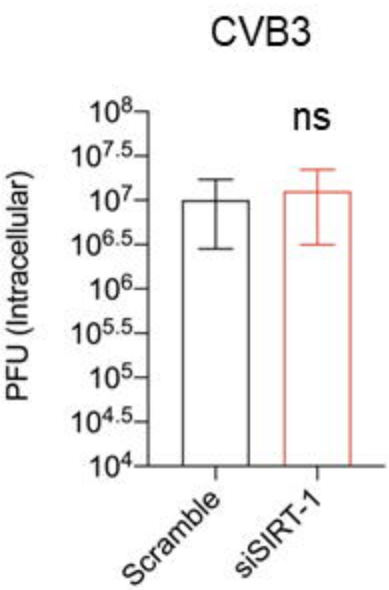

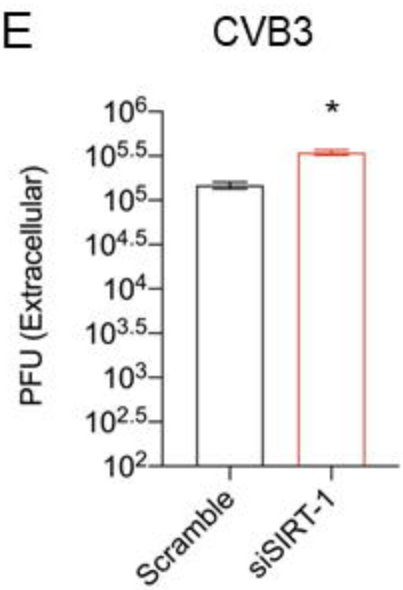
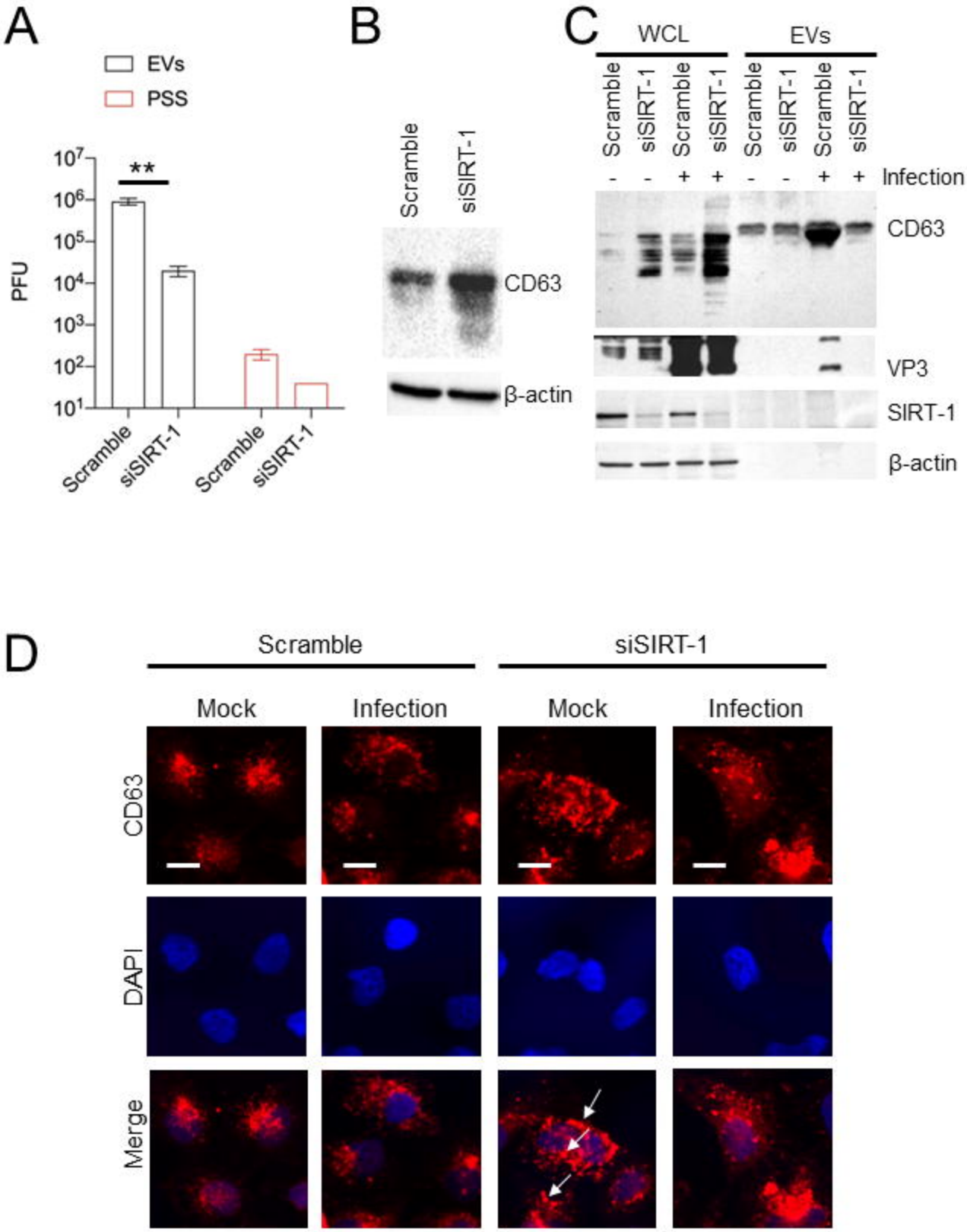
Fig. 6 SIRT-1 KD reduces Extracellular vesicle-mediated release of infectious EV-D68 viral particles